J Mol Model (2009) 15:349–355
DOI 10.1007/s00894-008-0405-x

ORIGINAL PAPER

In-silico screening of new potential Bcl-2/Bcl-xl inhibitors as apoptosis modulators

Anna Maria Almerico · Marco Tutone · Antonino Lauria

Received: 3 June 2008 / Accepted: 7 July 2008 / Published online: 6 December 2008

Abstract One of the major problems in the fight against cancer is drug-resistance, which, at a molecular level, can be acquired through mutations able to deactivate apoptosis. In particular, proteins in the Bcl-2 family are central regulators of programmed cell death, and members that inhibit apoptosis, such as Bcl-xl and Bcl-2, are overexpressed in many tumours. The development of new inhibitors of these proteins as potential anticancer therapeutics represents a new frontier. In this work, we carried out an in-silico screening of compounds from a free database of more than 2 million structures (ZINC database), which allowed us to identify 17 sulfonamide derivatives as new potential inhibitors; these are currently undergoing biological evaluation.

Keywords Apoptosis · Bcl-2 · Bcl-xl · Inhibitors · Molecular docking

Introduction

Proteins in the Bcl-2 family are central regulators of apoptosis [1], and members of this family that inhibit programmed cell death, such as Bcl-xl and Bcl-2, are overexpressed in many tumours and contribute to cancer onset, development, and resistance to therapy [2]. Members of the Bcl-2 family can be divided into pro-apoptotic and anti-apoptotic proteins. Pro-apoptotic members can be further divided into two groups: those that contain three Bcl homology (BH) domains (BH1–BH3), such as Bax, and Bak; and those that contain a single BH3 domain (BH3-only proteins), such as Bad, Bik, Bid, Bim, Hrk, Bmf, Noxa, and Puma. These proteins spread the cell death signal by inducing permeabilisation of the mitochondrial membrane, release of cytochrome *c*, and activation of a group of intracellular caspases. The resulting proteolytic cascade leads to cellular death. Anti-apoptotic Bcl-2 family members contain four BH domains (BH1–BH4) and include Bcl-2, Bcl-xl, Bcl-w, Mcl-1, and Bcl-2A1. These proteins have a protecting effect by binding their pro-death counterparts, and the cancer cells thus escape their death sentence. Inhibition of these anti-apoptotic proteins should specifically target the abnormal cell death pathway found in cancer cells, and offer an appealing target for therapeutic involvement. Thus, inhibiting anti-apoptotic Bcl-2 proteins holds promise as a means of improving therapeutic benefits and overcoming drug resistance in cancer treatment.

Structural studies of a Bcl-xl complex protein and the pro-apoptotic peptide Bak have revealed a hydrophobic cleft on Bcl-xl protein as the binding pocket for the pro-apoptotic peptide [3]; molecules binding to that hydrophobic cleft may overcome the protective effect that Bcl-xl exerts on the tumour cells. Following the logic of this statement has led to the recent discovery of many small molecules able to bind the hydrophobic cleft of Bcl-xl or Bcl-2 proteins. To date, three compounds demonstrated to interact better with these anti-apoptotic proteins, and mimic pro-apoptotic proteins, have reached clinical trials (Gossypol, ABT-737, GX015-070, Fig. 1), but none are yet available for therapeutic treatment. The aim of this work was to identify new potential inhibitors of this protein–protein interaction, starting from the structural features of the three cited compounds. Although there is no obvious structural similarity among these inhibitors, we selected a

A. M. Almerico (✉) · M. Tutone · A. Lauria
Dipartimento Farmacochimico, Tossicologico e Biologico,
Università degli Studi di Palermo,
Via Archirafi 32,
90123 Palermo, Italy
e-mail: almerico@unipa.it

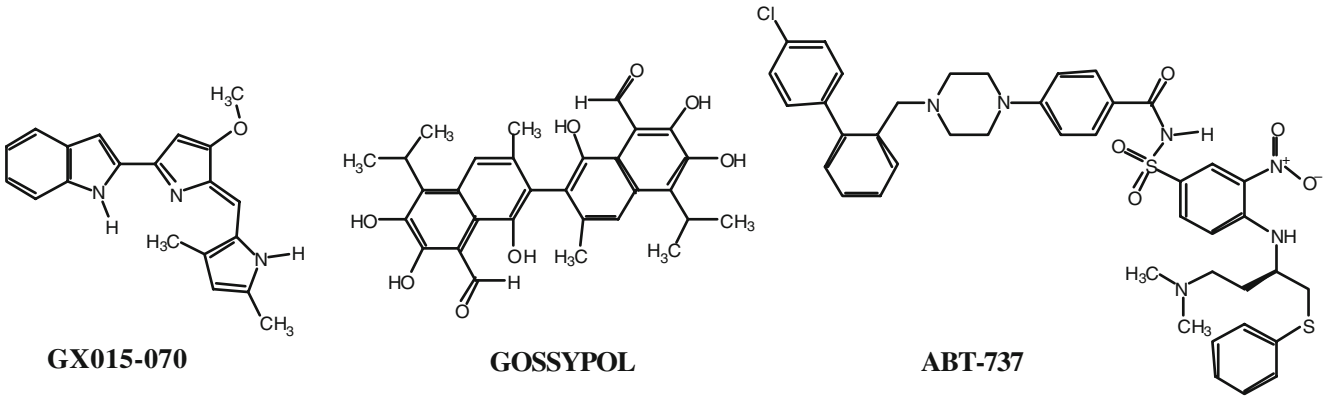

Fig. 1 Chemical structures of Bcl-xl / Bcl-2 inhibitors in clinical trials

set of molecular descriptors that provided guidelines with which to query a freely available database of more than 2 million structures, and carried out molecular docking and pharmacophoric studies on the hits obtained.

Materials and methods

Compound library creation

Structures were extracted from ZINC [4], a free database of commercially available compounds for virtual screening (see below).

Protein setup and ligand-based active site detection

For our purposes, we used the NMR-minimised average structure of the Bcl-xl/Bak peptide complex (1BXL) from the Brookhaven protein data bank (PDB; http://www.rcsb.org/). To identify and select the protein active site, Ligandfit by Accelrys, was used [5]. Ligandfit involves the use of a flood-filling algorithm that begins by constructing a rectangular grid with a user-defined spacing. In this investigation, the grid spacing was set as default (0.5 Å). Each grid point was then classified as either an occupied or a free point. Occupied grid points are those that lie within the contact distance of the nearest protein atom. The contact distance is set equal to the radius of the protein atom. The radius of each protein heavy atom is set at 2.5 Å, while the radius for protein hydrogen atoms is set at 2.0 Å. Grid points lying outside contact distance are free (unoccupied). An "eraser", which determines the opening size of the site, then removes the free grid points lying outside the protein, retaining the entire cavity found, which contains a specified number of free points. The utility of Ligandfit based on the presence of a known ligand pose was used: all free grid points that lie within the radius of any ligand atom were determined. Using the present endogen ligand (Bak), we carried out a ligand-based search for active sites (Docked Ligand mode).

Docking settings and scoring docked ligands

Docking calculations were carried out using the Monte Carlo method for a ligand conformational search. During the search, bond lengths were fixed; rotatable bonds were allowed to rotate freely. The number of trials for the Monte

Table 1 Calculated molecular descriptors for three known inhibitors. *MW* Molecular weight (Da), *cLog P* calculated Log P, *NRB* number of rotatable bonds, *HBD* H-bond donor, *HBA* H-bond acceptor, *SASA* solvent accessible surface area (Å^2), *AP* apolar desolvation (cal/mol) ($\Delta G = -\gamma$ SASA; γ=24 cal/mol/Å^2)[13], *PSA* polar surface area (Å^2)

Descriptor	ABT-737	Gossypol	GX015070
MW	813.50	518.60	317.42
cLog P	7.50	6.70	1.32
NRB	15	5	4
HBD	2	6	2
HBA	7	8	2
SASA	360.5	504.58	359.96
AP	−8.54	−12.109	−8.369
PSA	147.9	187.4	51

Table 2 Selection of filter values

		Molecular feature		
1.32	≤	cLogP	≤	7.5
4	≤	NRB	≤	15
2	≤	HBD	≤	6
2	≤	HBA	≤	8
−12.1	≤	AP	≤	−8.37
51	≤	SASA	≤	187.4
317	≤	MW	≤	814

Table 3 Docking results and consensus scores for the known inhibitors (Gossypol, ABT-737, and GX015-070) and the 17 selected hits

ZINC code	Dock score	Ligscore1	Ligscore2	PLP1	PLP2	PMF	Consensus
00828403	117.295	2.77	5.06	52.95	53.42	104.18	6
01093553	169.027	2.79	5.04	59.59	61.94	106.12	6
01112945	139.628	2.55	4.75	60.47	61.15	113.54	6
01399215	128.624	2.99	5.34	69.32	68.22	109.76	6
02336390	161.338	2.65	5.08	52.11	55.72	125.71	6
02952637	124.465	2.78	4.99	59.53	59.03	116.38	6
03017827	113.498	3.27	5.38	60.92	59.66	119.68	6
03170711	118.023	3.42	5.44	60.71	61.36	121.64	6
03225670	116.084	3.85	5.44	55.20	59.47	127.71	6
03230589	151.542	2.51	4.92	52.35	52.68	110.11	6
03300146	207.366	3.23	5.49	52.95	52.64	124.09	6
03336378	111.077	2.76	4.92	54.06	52.78	124.27	6
03660864	118.922	2.93	5.04	52.67	51.99	112.43	6
04352892	118.399	2.75	5.34	65.48	60.69	150.59	6
05433867	129.454	3.18	5.43	57.94	55.1	106.82	6
06577840	132.136	2.82	5.11	56.31	50.48	111.79	6
06973945	147.249	2.85	4.83	59.04	57.83	103.03	6
Gossypol	67.7352	3.46	5.41	60.27	58.21	134.11	5
ABT-737	58.3536	4.76	6.47	67.18	70.08	98.95	4
GX015-070	34.7725	1.14	3.81	43.49	40.89	104.23	1

Carlo search was fixed at 10,000, the maximum number of conformers saved was 10, and each conformer was classified as different from another if the root mean square deviation (RMSD) value was ≤ 1.50. In the calculation of ligand internal energy, electrostatic energy beyond the van der Waals energy (CFF1.02 force field) was also included. Both contributors were computed using 9-6 Lennard-Jones functions. For the docking energy calculation, the softened Lennard-Jones potential, with a tri-linear interpolation and a rigid body minimisation of the non-bonded interaction energy between the ligands and the protein, was used [6]. The final docked energy was calculated as the sum of the intermolecular energy and the internal energy of the ligand.

The Ligandfit protocol employs scoring functions to prioritise docked ligands relative to one another, and to predict binding affinities. The pool of available scoring functions includes Dock Score [5], LigScores1 and 2 [6], PLP1 [7, 8] and 2 [9], and PMF [10].

Table 4 Calculated molecular descriptors for the 17 selected hits. See for Table 1 for definitions

ID	cLogP	AP	PSA	HBD	HBA	MW	NRB
1	4.11	−9.46	−21.9	2	7	518.616	8
2	3.8	−10.16	−22.58	3	8	528.439	8
3	2.96	−9.49	−18.41	2	8	476.576	10
4	4.00	−8.83	−15.81	2	6	417.899	4
5	1.89	−11.04	−16.99	2	8	440.543	10
6	4.28	−8.93	−23.73	2	7	520.632	10
7	4.78	−8.95	−20.23	2	8	552.74	11
8	3.39	−8.38	−21.03	2	8	520.673	6
9	4.22	−8.73	−46.07	1	8	518.662	7
10	4.40	−8.98	−58.41	3	8	539.703	8
11	3.78	−8.69	−18.4	2	8	501.63	8
12	2.06	−9.01	−23.56	2	8	425.532	8
13	5.27	−8.45	−23.74	2	7	536.675	10
14	5.33	−8.59	−15.35	2	6	544.698	6
15	3.58	−9.65	−15.57	2	8	494.598	6
16	1.94	−8.87	−20.68	3	8	457.525	8
17	2.64	−8.60	−15.28	2	8	410.521	6

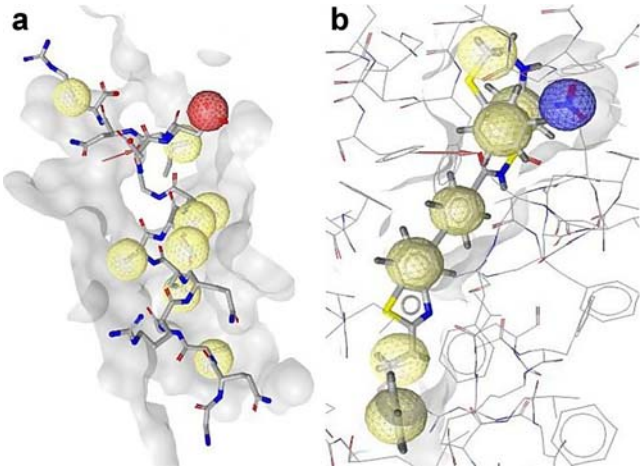

Fig. 2 Pharmacophoric features of Bak (**a**) and ABT-737 (**b**). *Yellow* hydrophobic regions, *red* negative ionisable volume, *blue* positive ionisable volume

To rapidly identify ligands that score highly in more than one scoring function, consensus scoring [6] was employed; a rank score of 1 was assigned to the top 10% scoring molecules for a given score and a rank score of 0 to the remaining molecules.

Pharmacophoric analysis

Ligandscout [11] software was employed to investigate pharmacophoric features. The following chemical features were taken into account: hydrogen bond interactions; electrostatic fluor-hydrogen bond donor interaction; hydrophobic areas, distinguishing between aliphatic and aromatic (pi-stacking) interactions; charge–transfer interactions, which are divided into positively ionisable areas represented by atom or groups of atoms that are likely to be protonated at physiological pH, and negatively ionisable areas that are likely to be deprotonated at physiological pH.

Results and discussion

We began by analysing the molecular structures of three compounds currently in clinical trials (GX015-070, Gossypol, ABT-737). For each compound, a set of molecular descriptors was calculated: cLog P, number of rotatable bonds (RB), number of H-bond donors (HBD) and H-bond acceptors (HBA), apolar desolvation (AP), polar surface area (PSA), molecular weight (MW) and solvent accessible surface area (SASA) (Table 1). Analysis of descriptors shows that these compounds do not strictly respect Lipinski's rule of five [12]. ABT-737 and Gossypol have MW > 500 and cLog P > 5, and again ABT-737, one of the promising candidate to therapy has an RB > 5.

Lipinski's rule of five describes molecular features important for a drug's pharmacokinetics in the human body, including their absorption, distribution, metabolism, and excretion (ADME). However, the rule cannot predict if a compound is pharmacologically active. In recent years, this rule was used in virtual high-throughput screenings as a filter to broadly discriminate compounds, but in this work we decided to use as filters the range of descriptors values of the three known inhibitors already defined for the target Bcl-2/Bcl-xl (Table 2). This choice was based on the consideration that Lipinski's rule of five is a rule-of-thumb to evaluate "drug-like-ness", or to determine if a chemical compound with a certain pharmacological or biological activity has properties that would make it likely to be an orally active drug in humans.

Therefore, the parameter ranges listed in Table 2 were used to sift the ZINC database—a library of more than 2 million molecules—and the search was restricted to commercially available compounds.

Our search identified 2,229 potential candidates, with already optimised structures, which were then subjected to docking analysis. The consensus score for each scoring function, taking the consensus obtained for gossypol (5) as the cut-off value, ranked 17 of the 2,229 compounds better than the three sample molecules (Table 3).

All the candidates identified belong to the sulfonamide class, and in some cases bear more than one sulfonamide group. From the descriptors point of view, it is worth noting that there are some violations of Lipinski's rule of five among the 17 sulfonamides, above all in terms of MW (several compounds exceed 500 Da), and only one candidate shows an RB < 5. Only in terms of HBD and HBA there are no violations, since two structures also present cLog P > 5. (Table 4).

In terms of pharmacophoric features, analysis of the endogen ligand Bak co-crystallised with Bcl-xl (PDB: 1BXL) showed the presence of nine hydrophobic regions, confirming the lipophilic nature of the Bcl-xl binding pocket, one negative ionisable volume and the possibility of establishing an H-bond with the –OH of Tyr195 (Fig. 2a). The high number of hydrophobic regions is clearly due to the huge dimensions of Bak as a peptide. The search for Bcl-xl inhibitors pointed towards small organic molecules; in fact, when a pharmacophoric analysis was carried out on Bcl-xl crystallised with an inhibitor in clinical trials (ABT-737, PDB: 1YSN) (Fig. 2b), the number of hydrophobic regions decreased to seven, but the HBA is conserved and a positive ionisable region is present.

The 17 sulfonamides identified by the virtual screening, the structures of which are shown in Fig 3, exhibit similar pharmacophoric features (Fig. 4): a high number of hydrophobic regions, one HBA region and, in some cases, also an aromatic region able to interact via pi-stacking with

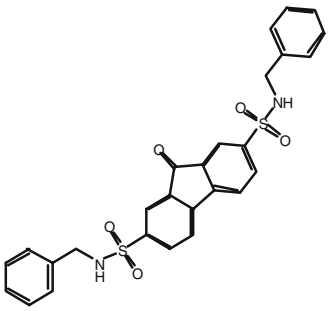

00828403 (**1**)

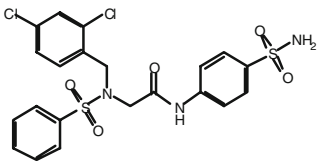

01093553 (**2**)

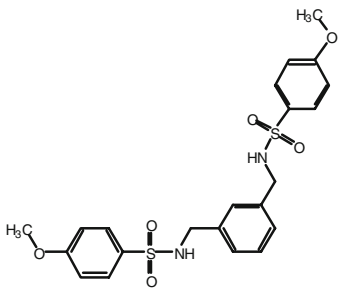

01112945 (**3**)

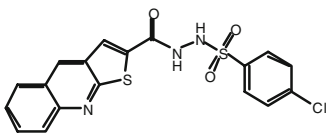

01399215 (**4**)

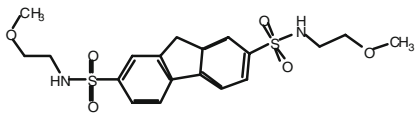

02336390 (**5**)

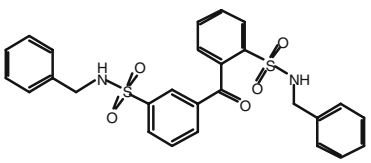

02952637 (**6**)

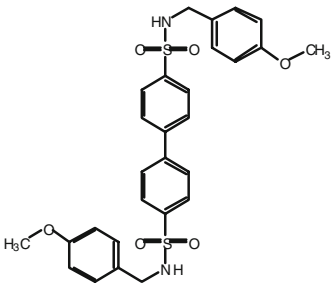

03017827 (**7**)

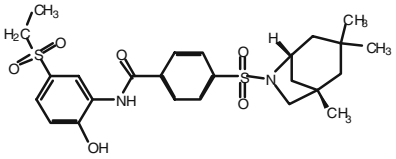

03170711 (**8**)

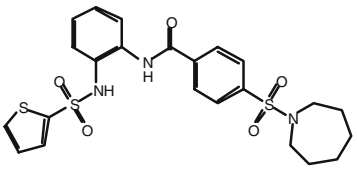

03225670 (**9**)

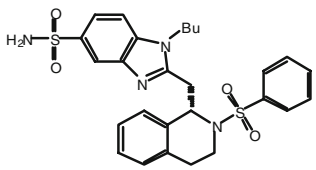

03230589 (**10**)

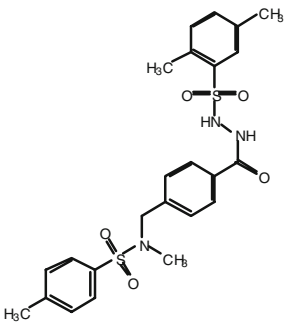

03300146 (**11**)

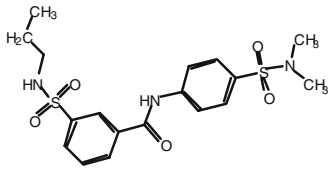

03336378 (**12**)

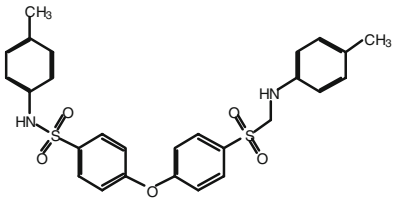

03660864 (**13**)

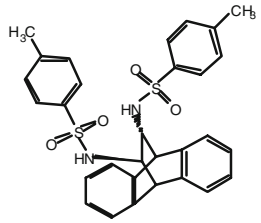

04352892 (**14**)

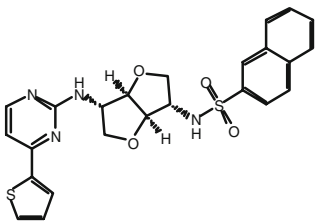

05433867 (**15**)

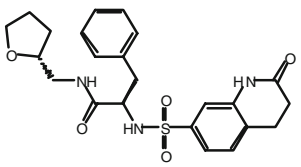

06577840 (**16**)

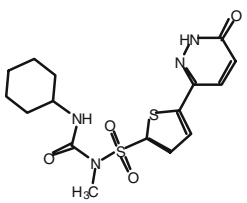

06973945 (**17**)

Fig. 3 Two-dimensional structures of selected inhibitors

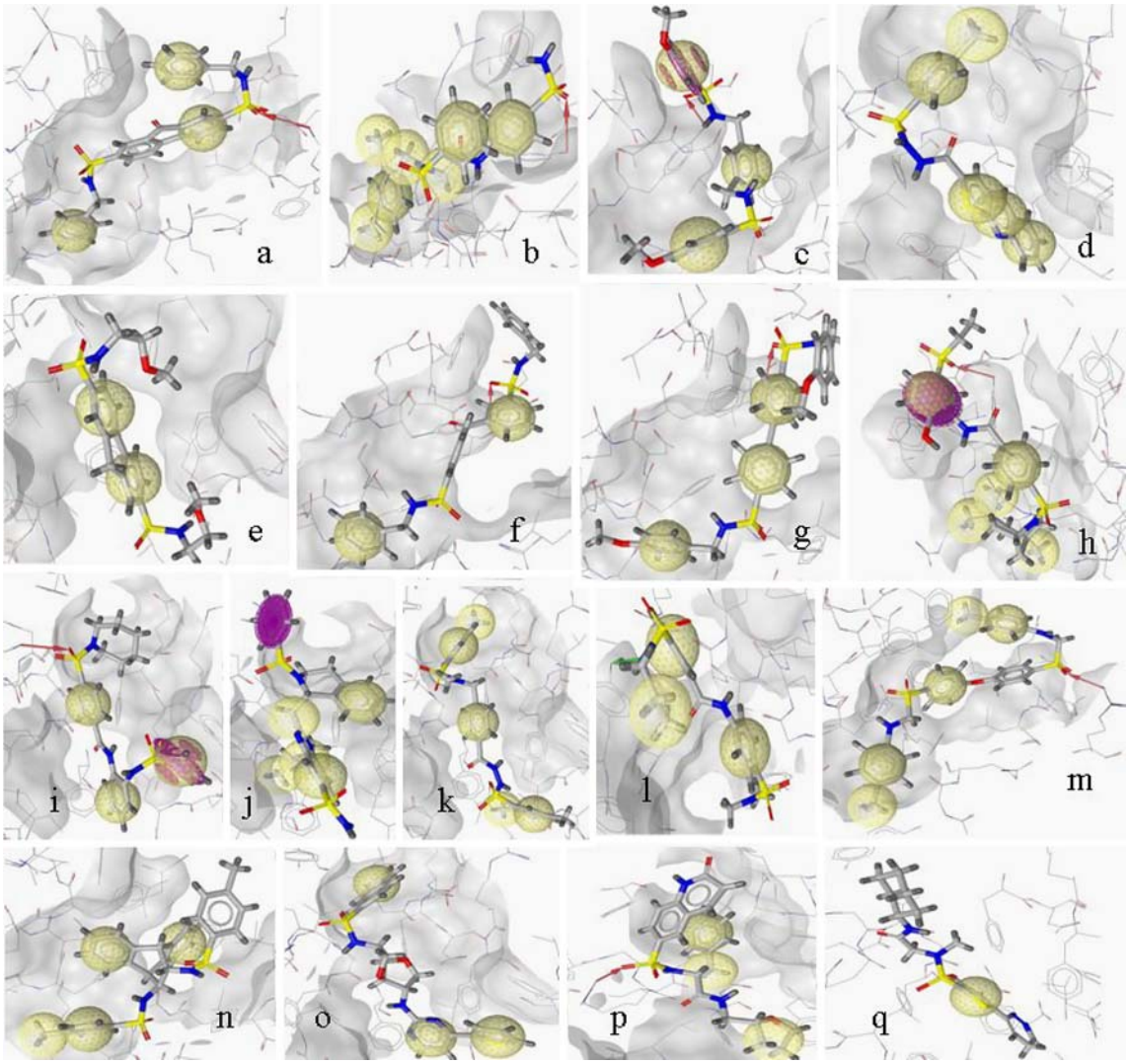

Fig. 4a–q Pharmacophoric features of the selected inhibitors. **a** ID1, **b** ID2, **c** ID3, **d** ID4, **e** ID5, **f** ID6, **g** ID7, **h** ID8, **i** ID9, **j** ID10, **k** ID11, **l** ID12, **m** ID13, **n** ID14, **o** ID15, **p** ID16, **q** ID17 (for colour coding, see Fig. 2)

aromatic amino acids such as Tyr195 or Phe105. The number of hydrophobic regions is generally not higher than seven (as in the case of ID2, Fig. 4b), and for most of these compounds is in the range of 3–5. Compounds ID17 and ID5 possess only one and two hydrophobic regions, respectively: the lipophilic volume of the binding pocket is occupied by a thiophene ring in the case of ID17 (Fig. 4q) and by the phenyl rings of a fluorene moiety in the case of ID5 (Fig. 4e). It is interesting to note that 10 out of 17 sulfonamide derivatives establish H-bonds. In nine cases this is an HBA due to the oxygen of one of the sulfonamide groups, which interacts with –OH of Tyr101, with Arg132 (ID1), or Arg139 (ID9 and ID16). Only in one case, ID12, is an HBD present, but the amino acid involved remains Tyr101. In addition to the features discussed above, three derivatives (ID3, ID8, ID9) exhibit a hydrophobic feature sphere because of a pi-stacking interaction of the phenyl ring with the same amino acid (Phe105).

The 17 sulfonamide derivatives identified are currently under investigation for biological screening tests that should confirm our findings. This methodology has the great advantage that the drug candidates are all commercially available, thus it is possible to avoid time-consuming synthetic pathways.

Conclusions

In this work we carried out a virtual screening of new potential Bcl2/Bcl-xl inhibitors starting from an analysis of the structural features of the three compounds (Gossypol, GX015-070, and ABT-737) currently in clinical trials.

This search allowed us to identify 17 sulfonamide derivatives, from a starting library of 2,229 molecules, which showed better docking scores than Gossypol, GX015-070, and ABT-737. These compounds can therefore be expected to possess a high inhibition capability, and their K_i should be higher than those measured for ABT-737 and other isomers discovered through the active analog approach and recently proposed as Bcl-2 inhibitors [14]. Furthermore, the compounds selected here revealed pharmacophoric features that fit well with the Bcl-xl binding pocket, also satisfying the requirements evidenced in NMR-derived complex structures [15]. And last but not least, our methodology has the advantage that it deals with commercially available compounds, which thus do not require to be synthesised, which means a reduction of time and costs, a far from negligible factor in academic research.

References

1. Daniel NN, Korsmeyer SJ (2004) Cell 116:205–219. doi:10.1016/S0092-8674(04)00046-7
2. Kirkin V, Joos S, Zornis M (2004) Biochim Biophys Acta 1644:229–249. doi:10.1016/j.bbamcr.2003.08.009
3. Sattler M, Liang H, Nettesheim DN, Meadows RP, Harlan JE, Eberstadt M et al (1997) Science 275:983–986. doi:10.1126/science.275.5302.983
4. Irwin JJ, Shoichet BK (2005) J Chem Inf Model 45:177–182. doi:10.1021/ci049714 +
5. Ligandfit User Manual, Accelrys Inc, 2003.
6. Venkatachalam C, Jiang X, Oldfield T, Waldman M (2003) J Mol Graph Model 21:289–307. doi:10.1016/S1093-3263(02)00164-X
7. Verkhivker G, Bouzida D, Gehlhaar DB, Rejto P, Arthurs S, Colson A et al (2000) J Comput Aided Mol Des 14:731–751. doi:10.1023/A:1008158231558
8. Gehlhaar D, Verkhivker G, Rejto P, Sherman C, Fogel D, Fogel L et al (1995) Chem Biol 2:317–324. doi:10.1016/1074-5521(95)90050-0
9. Gehlhaar D, Bouzida D, Rejto P (1999) Reduced dimensionality in ligand–protein structure prediction: covalent inhibitors of serine proteases and design of site-directed combinatorial libraries. In: Parrill AL, Reddy MR (eds) Rational drug design: novel methodology and practical applications, vol 719. American Chemical Society, Washington, DC, pp 292–311
10. Muegge I, Martin Y (1999) J Med Chem 42:791–804. doi:10.1021/jm980536j
11. Wolber G, Langer T (2005) J Chem Inf Model 45:160–169. doi:10.1021/ci049885e
12. Lipinski CA, Lombardo F, Dominy BW, Feeney PJ (2001) Adv Drug Deliv Rev 46:3–26. doi:10.1016/S0169-409X(00)00129-0
13. Cheng A, Coleman R, Smyth K, Cao Q, Soulard P, Caffrey D et al (2007) Nat Biotechnol 25:71–75. doi:10.1038/nbt1273
14. Bruncko M, Oost TK, Belli BA, Ding H, Joseph MK, Kunzer A et al (2007) J Med Chem 50:641–662. doi:10.1021/jm061152t
15. Oltersdorf T, Elmore SW, Shoemaker AR, Armstrong RC, Augeri DJ, Belli BA et al (2005) Nature 435:677–681. doi:10.1038/nature03579